INSTITUTE OF PHYSICS PUBLISHING SMART MATERIALS AND STRUCTURES
Smart Mater. Struct. **12** (2003) 57–64 PII: S0964-1726(03)56151-1

Reducing the inductance requirements of piezoelectric shunt damping systems

A J Fleming[1], **S Behrens and S O R Moheimani**

School of Electrical Engineering and Computer Science, University of Newcastle, Callaghan 2308, Australia

E-mail: andrew@ee.newcastle.edu.au

Received 27 November 2001, in final form 16 August 2002
Published 10 January 2003
Online at stacks.iop.org/SMS/12/57

Abstract
Structural vibration can be reduced by shunting an attached piezoelectric transducer (PZT) with an electrical impedance. Current shunt circuit designs, e.g. a single-mode inductor–resistor network, typically require large inductance values of up to thousands of henries. In practice, discrete inductors are limited in size to around 1 H. By placing an additional capacitance across the terminals of the PZT, shunt circuit inductances can be drastically reduced. To justify our claims, we present a theoretical analysis of the damped system and identify the influence of the additional capacitance. Two modes of a simply supported beam are successfully damped using a capacitance modified shunt circuit. A low inductance multi-mode circuit is also studied and experimentally verified.

1. Introduction

By shunting a structurally attached piezoelectric transducer (PZT) with a passive electrical network, mechanical energy can be dissipated from the host structure. The design of shunt damping circuits has been heavily studied in the literature since the original contributions by [14] and [16]. A series inductor and resistor inductor–resistor (R–L) circuit was used to damp a single structural mode. This network, when combined with the inherent capacitance of a PZT, creates a damped electrical resonance, equivalent to that of a tuned vibrational energy absorber [16]. This damping methodology is commonly referred to as passive shunt damping. One highly sought-after characteristic in vibration control systems is that of guaranteed stability in the presence of structural uncertainties. This quality results naturally from the fundamental properties of passive shunt damping systems [23, 24].

Piezoelectric shunt damping circuits typically require the use of large inductances (up to thousands of henries). Virtual grounded and floating inductors (Riordan gyrators [26]) are required to implement the inductor elements. Such virtual implementations are generally poor representations of ideal inductors. They are large in size, difficult to tune, and are sensitive to component variations. Virtual circuit implementations also require an external power source and a large number of costly high voltage components [12, 13]. Recently, a new method has been presented for implementing piezoelectric shunt damping circuits [11, 12]. The *synthetic admittance*, consisting of a voltage controlled current source and signal filter, is capable of implementing any proper admittance transfer function. The circuit contains very few high voltage components but still requires an external power supply.

In an attempt to eliminate the need for large inductors, a literature has also developed on the so-called *switched shunt* or *switched stiffness* techniques [7]. Three major subclasses exist where the piezoelectric element is switched in and out of a shunt circuit comprising either another capacitor [8], a resistor [6], or an inductor [25]. The required inductance is typically one tenth that required to implement a simple L–R resonant shunt circuit designed to damp the same mode. To their detriment, such techniques are applicable only to single degree of freedom structures or structures with sinusoidal excitation. As with virtual circuit implementation, an external power source is required for the gate drive and timing electronics.

This paper is aimed at reducing the inductance requirements of piezoelectric shunt damping circuits. By placing an additional capacitance across the terminals of the PZT the effective piezoelectric capacitance can be increased. This technique is beneficial to all shunt circuits containing

[1] Author to whom any correspondence should be addressed.

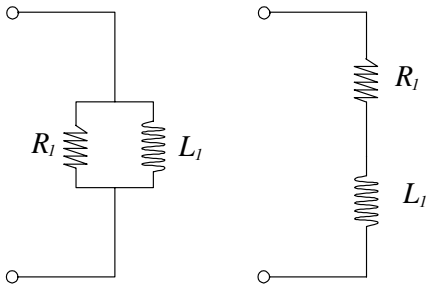

Figure 1. Single-mode shunt damping circuits.

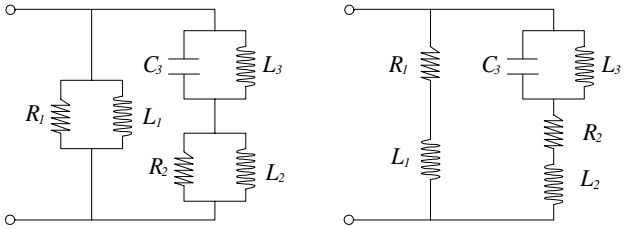

Figure 2. Parallel and series multi-mode shunt circuits.

inductors whose values are inversely proportional to the piezoelectric capacitance. At the present time, this covers all resonant shunting techniques. In addition, the inductance of hybrid switching circuits [7] is also loosely related to the inverse of piezoelectric capacitance. Increasing the effective piezoelectric capacitance results in shunt circuits with smaller inductance values. A quantifiable performance penalty is involved.

A new piezoelectric multi-mode shunt damping structure is also introduced. The *series–parallel* impedance structure uses less components, and contains smaller inductors than most previous circuit designs.

This paper is presented in five sections. We begin with a brief review of single- and multi-mode piezoelectric shunt circuit design. In section 3 we discuss the modelling of PZTs and show how to model the presence of an electrical shunt impedance. The effect of an additional piezoelectric capacitance is modelled in section 4. The multi-mode series–parallel impedance structure is introduced in section 5. Experimental results are presented in section 6. We conclude with a review of the initial goals and a summary of the theoretical and experimental results.

2. Piezoelectric shunt damping

Shunt damping methodologies are often grouped into two broad categories: single mode and multi-mode. Single-mode shunt damping techniques are simple, but damp only one structural mode for every PZT. Multiple-mode shunt damping techniques require more complicated shunt circuits but are capable of damping many modes.

2.1. Single-mode shunt damping

Single-mode damping was introduced to decrease the magnitude of one structural mode [14, 18]. Two examples of single-mode damping are shown in figure 1; parallel and series shunt damping. An R–L shunt circuit introduces an electrical resonance. This can be tuned to one structural mode in a manner analogous to a mechanical vibration absorber. Single-mode damping can be applied to reduce several structural modes with the use of as many piezoelectric patches and damping circuits as necessary.

Problems may result if these piezoelectric patches are bonded to, or embedded in the structure: first, the structure may not have sufficient room to accommodate all of the patches; and second, the structure may be altered or weakened when the piezoelectric patches are applied. In addition, a large number of patches can increase the structural weight, making it unsuitable for applications such as aerospace systems and structures.

2.2. Multiple-mode shunt damping

To alleviate the problems associated with single-mode damping, multi-mode shunt damping has been introduced, i.e. the use of one piezoelectric patch to damp several structural modes.

One methodology for multi-mode shunt damping is to insert a *current blocking* circuit [28–31] in series with each shunt branch. In figure 2, the blocking circuit consists of a capacitor and an inductor in parallel, C_3–L_3. The number of antiresonant circuits in each R–L shunt branch depends on the number of structural modes to be damped simultaneously. Each R–L shunt branch is designed to damp one structural mode. For example, R_1–L_1 in figure 2 is tuned to resonate at ω_1, the resonant frequency of the first structural mode to be damped. R_2–L_2 is tuned to ω_2, the second structural mode to be damped, and so on.

According to Wu [29], the inductance values for the shunt circuits shown in figure 2 can be calculated from the following expressions (it is assumed that $\omega_1 < \omega_2$):

$$L_1 = \frac{1}{\omega_1^2 C_p} \qquad \tilde{L}_2 = \frac{1}{\omega_2^2 C_p} \qquad L_3 = \frac{1}{\omega_1^2 C_3}$$
$$L_2 = \frac{(L_1\tilde{L}_2 + \tilde{L}_2 L_3 - L_1 L_3 - \omega_2^2 L_1 \tilde{L}_2 L_3 C_3)}{(L_1 - \tilde{L}_2)(1 - \omega_2^2 L_3 C_3)} \tag{1}$$

where C_p is the capacitance of the PZT, and C_3 is an arbitrary capacitor used in the current blocking network. In the following sections C_3 will be taken as 100 ηF.

More recently, the *current flowing* shunt circuit has been introduced [3, 4]. Shown in figure 3, the current flowing circuit requires one circuit branch for each structural mode to be controlled. The current flowing $\hat{L}_i$–C_i network in each branch is tuned to approximate a short circuit at the target resonance frequency whilst approximating an open circuit at the adjacent branch frequencies. The remaining inductor and resistor in each branch $\tilde{L}_i$–R_i, is tuned to damp the ith target structural mode in a manner analogous that performed during single-mode design. That is, the current flowing network decouples the multi-mode problem into a number of approximately independent single-mode designs. Unlike current blocking techniques, the order of each current flowing branch does not increase as the number of modes to be shunt-damped simultaneously increases. Besides greatly simplifying the tuning procedure, the current flowing technique requires less

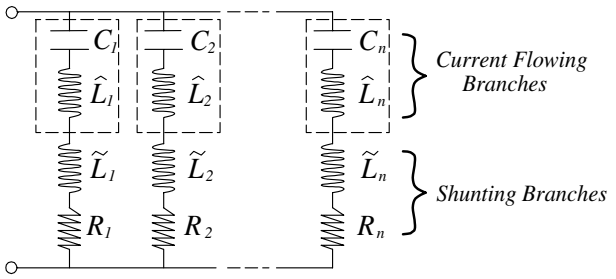

Figure 3. The current flowing shunt circuit.

components and gracefully extends to damp a large number of modes simultaneously, e.g. five modes of a simply supported plate [4]. Further practical advantages are realized when implementing the circuit: only a single non-floating inductor is required per branch [4]. A similar technique can be found in [19].

Other single- and multi-mode shunt damping methods have also been developed. As an active technique, the negative capacitance approach [1] has been employed to suppress structural and acoustic vibration [32]. Simple resistors have also been demonstrated to provide a small amount of damping [16]. As this paper is dedicated to resonant shunt circuits, and the two previously mentioned techniques do not include inductors, such techniques will be discussed no further.

3. Modelling the compound system

For generality, we will enter the modelling process with knowledge *a priori* of the system dynamics. As an example we consider a simply supported beam with two bonded piezoelectric patches, one to be used as a source of disturbance, and the other for shunt damping. The transfer function $G_{vv}(s)$, measured from applied actuator to sensor voltage can be derived analytically from the Euler–Bernoulli beam equation [15]. Alternatively, this transfer function can be obtained experimentally through system identification [21]. Using similar methods, we also consider the transfer function measured from the applied actuator voltage to displacement at a point $G_{yv}(x, s)$.

Following the modal analysis procedure [22], the resulting transfer functions have the familiar form

$$G_{yv}(x,s) \triangleq \frac{Y(x,s)}{V_a(s)} = \sum_{i=1}^{\infty} \frac{F_i \phi_i(x)}{s^2 + 2\zeta_i w_i s + w_i^2} \tag{2}$$

$$G_{vv}(s) \triangleq \frac{V_s(s)}{V_a(s)} = \sum_{i=1}^{\infty} \frac{\alpha_i}{s^2 + 2\zeta_i w_i s + w_i^2} \tag{3}$$

where F_i, and α_i represent the lumped modal and piezoelectric constants applicable to the ith mode of vibration.

3.1. Piezoelectric modelling

Piezoelectric crystals have a three-dimensional structure, i.e. crystal deformation occurs in three dimensions. Practical mechanical applications require the effect in one or two dimensions only, which can be achieved by manufacturing piezoelectric patches with large length and width to thickness ratios.

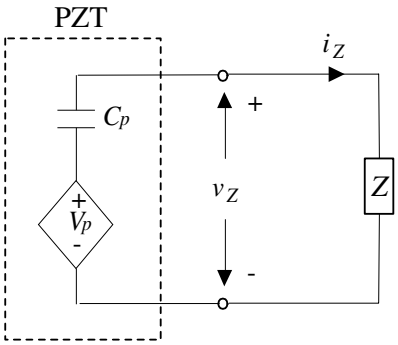

Figure 4. Equivalent electrical model of a PZT.

PZTs behave electrically like a capacitor and mechanically like a stiff spring [20]. An equivalent electrical model has been presented [9, 10, 16, 27] and is widely used in the literature. The model, shown in figure 4, consists of a strain-dependent voltage source and series capacitor.

3.2. Modelling the presence of a shunt circuit

Consider figures 4 and 5 where a piezoelectric patch is shunted by an impedance Z. The current–voltage relationship can be represented in the Laplace domain as

$$V_z(s) = I_z(s) Z(s) \tag{4}$$

where $V_z(s)$ is the voltage across the impedance and $I_z(s)$ is the current flowing through the impedance. Using Kirchhoff's voltage law on the circuit shown in figure 4 we obtain

$$V_z(s) = V_p(s) - \frac{1}{C_p s} I_z(s) \tag{5}$$

where V_p is the voltage induced by the electromechanical coupling effect [16] and C_p represents the capacitance of the shunting layer. Combining (4) and (5) we obtain

$$V_z(s) = \frac{Z(s)}{\frac{1}{C_p s} + Z(s)} V_p(s) \tag{6}$$

or

$$V_z(s) = \frac{C_p s Z(s)}{1 + C_p s Z(s)} V_p(s). \tag{7}$$

Notice that when $Z = \infty$, i.e. open circuit, we have

$$Z = \infty \quad \Rightarrow \quad V_z(s) \triangleq V_p(s) = G_{vv}(s) V_a(s). \tag{8}$$

However, if the circuit is shunted by Z, we can assume that

$$V_p(s) = G_{vv}(s) V_a(s) - G_{vv}(s) V_z(s) \qquad \text{s.t. } Z \neq \infty, 0. \tag{9}$$

The above equations (8) and (9) are reported in state-space form [17] as the *sensing* and *actuator equations*. By substituting (6) into (9),

$$V_p(s) = G_{vv}(s) V_a(s) - G_{vv}(s) \frac{Z(s)}{\frac{1}{C_p s} + Z(s)} V_p(s) \tag{10}$$

and rearranging we find the shunt damped transfer function

$$\frac{V_p(s)}{V_a(s)} = \frac{G_{vv}(s)}{1 + G_{vv}(s) K(s)} \tag{11}$$

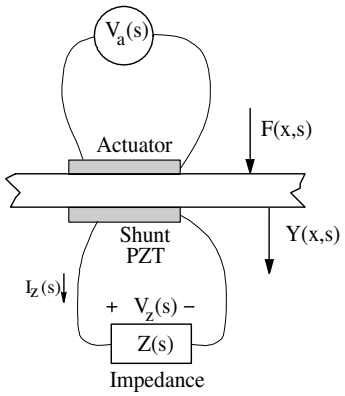

Figure 5. Structural inputs/outputs.

where

$$K(s) = \frac{Z(s)}{Z(s) + \frac{1}{C_p s}}. \tag{12}$$

Note that $V_p(s)$ is dynamically equivalent to $V_s(s)$ (i.e. the open circuit voltage). We can rewrite the shunt-damped or closed loop transfer functions as

$$\tilde{G}_{vv}(s) \triangleq \frac{V_s(s)}{V_a(s)} = \frac{G_{vv}(s)}{1 + G_{vv}(s)K(s)} \tag{13}$$

and

$$\tilde{G}_{yv}(x, s) \triangleq \frac{Y(x, s)}{V_a(s)} = \frac{G_{yv}(x, s)}{1 + G_{vv}(s)K(s)}. \tag{14}$$

From equations (13) and (14) we observe that shunt damping is equivalent to a negative feedback control strategy parameterized in terms of the shunt impedance $Z(s)$.

Using a similar procedure and the principle of superposition, the effect of a generally distributed disturbance force can be included:

$$V_s(s) = \frac{G_{vf}(s)F(x, s)}{1 + K(s)G_{vv}(s)} + \frac{G_{vv}(s)V_{in}(s)}{1 + K(s)G_{vv}(s)} \tag{15}$$

$$Y(x, s) = \frac{G_{yf}(x, s)F(x, s)}{1 + K(s)G_{vv}(s)} + \frac{G_{yv}(x, s)V_{in}(s)}{1 + K(s)G_{vv}(s)}. \tag{16}$$

4. Supplementary capacitance

The foremost problem with shunt damping implementation is the large required inductances.

Consider a shunt circuit employed to damp a single structural mode centered at 100 Hz, assuming a typical PZT capacitance of 100 nF, and required inductance 25.3 H. To implement such inductance values, designers have turned to the use of opamp based virtual inductors and, more recently, impedance synthesizing devices [11–13]. In many circumstances, it may be undesirable to use such methods as they introduce additional complexity, reliability issues, and require external power sources.

By noting that the inductance values (1) are inversely proportional to the equivalent piezoelectric capacitance, inductances can be reduced by simply increasing the capacitance. This is achieved by selecting a PZT with higher dielectric constant, lesser thickness, or greater surface area.

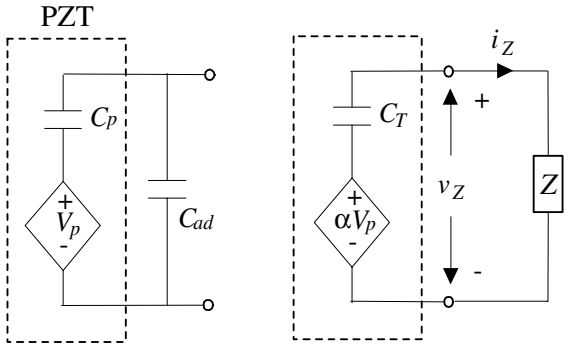

Figure 6. Electrical and Thevénin equivalent model of the PZT with additional parallel capacitance.

Alternatively, the piezoelectric capacitance can be increased by placing an additional capacitance C_{ad} in parallel with the PZT.

The effect of the additional capacitance can be modelled by considering the Thevénin equivalent network, figure 6. Parameters of the equivalent circuit are shown below (17):

$$C_T = C_p + C_{ad} \qquad \alpha = \frac{C_p}{C_p + C_{ad}}. \tag{17}$$

By following a procedure similar to that of section 3.2, a model of the compound system can be obtained. The network equation (6) is replaced with

$$V_z(s) = \frac{Z(s)}{\frac{1}{C_T s} + Z(s)} \alpha V_p(s). \tag{18}$$

This is substituted into (9), yielding the closed loop transfer function from applied actuator to piezoelectric sensor voltage $\tilde{G}_{vv}^{cap}(s)$:

$$\tilde{G}_{vv}^{cap}(s) \triangleq \frac{V_s(s)}{V_a(s)} = \frac{G_{vv}(s)}{1 + G_{vv}(s)\alpha K(s)} \tag{19}$$

$$K(s) = \frac{Z(s)}{Z(s) + \frac{1}{C_T s}}. \tag{20}$$

Similarly

$$\tilde{G}_{yv}^{cap}(x, s) \triangleq \frac{Y(x, s)}{V_a(s)} = \frac{G_{yv}(x, s)}{1 + G_{vv}(s)\alpha K(s)}. \tag{21}$$

For a series configuration single-mode shunt damping circuit (shown in figure 1), the structure of the feedback controller is as follows:

$$K(s) = \frac{Z(s)}{Z(s) + \frac{1}{C_p s}} \tag{22}$$

$$= \frac{L_1 C_p s^2 + R_1 C_p s}{L_1 C_p s^2 + R_1 C_p s + 1}. \tag{23}$$

If C_p is replaced with C_T, we wish to find component values that will retain the original feedback controller $K(s)$. Simply

$$\hat{L}_1 = L_1 \frac{C_p}{C_T} \qquad \hat{R}_1 = R_1 \frac{C_p}{C_T} \tag{24}$$

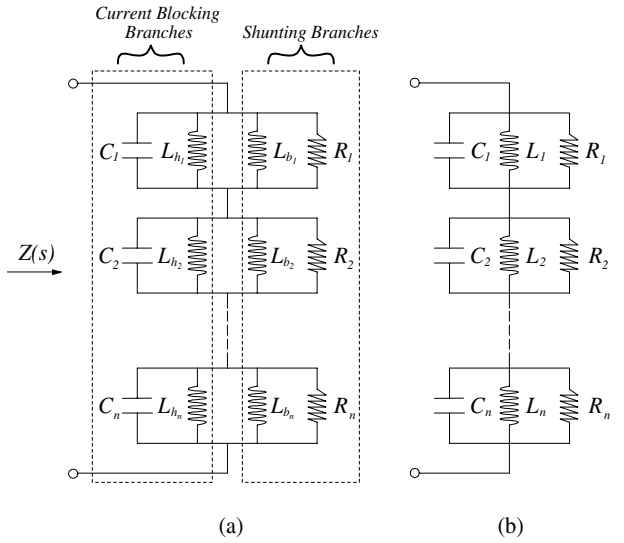

Figure 7. The series–parallel impedance structure (a), and simplified circuit (b).

where $\hat{L}_1$, and $\hat{R}_1$ are the shunt circuit components for use with C_T. Thus the inductance and resistance values are reduced by the same factor by which the capacitance is increased.

For multi-mode shunt circuits the result is similar. Because the PZT capacitance has increased, branch inductance and resistance values decrease. The inductors contained in the current blocking networks are not dependent on the PZT capacitance. The inductance is dependent on the arbitrary capacitance C_3, and hence is also arbitrary.

In summary, by artificially increasing the PZT capacitance, inductance values can be reduced but at the expense of damping performance. Supplementary capacitance has the effect of reducing the feedback controller gain $K(s)$. The exact performance loss, in terms of dB reduction, is a function of the open loop dynamics, the amount of additional capacitance, the structure of the shunt circuit, and the component values. For any specific case, samples of the expected performance loss must be found directly by simulation.

5. New multi-mode shunt damping structure

In this section, a new multimode piezoelectric shunt damping structure is presented. The *series–parallel* impedance structure contains significantly smaller inductors than other resonant shunt techniques.

Consider the series–parallel multimode impedance structure shown in figure 7(a). Each parallel network C_i–L_{h_i}–L_{b_i}–R_i contains two sub-networks: a current blocking network C_i–L_{h_i}, and a parallel single-mode shunt damping network L_{b_i}–R_i. As in [28], for a specific mode with resonance frequency ω_i, both the current blocking and shunt damping networks, C_i–L_{h_i} and L_{b_i}–C_p, are tuned to ω_i.

The operation is described fairly simply. At a specific structural resonance ω_i, the current blocking network tuned to that mode has an extremely large impedance. All other adjacent current blocking networks, tuned to the remaining structural resonance frequencies, have a low impedance at ω_i. Thus, a voltage applied at the terminals results in a current that flows freely through the detuned low impedance current blocking networks and through the shunt damping network connected in parallel to the current blocking network tuned to ω_i. In this way, the circuit is decoupled so that each damping network L_{b_i}–R_i–C_p, can be tuned individually to the target resonance frequency. At a structural resonance ω_i, the overall impedance is approximately L_{b_i}–R_i.

In its simplest form, as described above, the series–parallel structure offers no great advantages over current techniques. Although it contains less components than traditional current blocking networks [28, 30], the circuit is little more than the parallel dual of so-called current flowing techniques [3, 5]. Benefits arise from a suitable a choice in the arbitrary capacitances C_i. The recommended capacitance value is 10–20 times larger than the piezoelectric capacitance. In this case, the current blocking inductors will be significantly smaller than the damping inductors. As shown in figure 7(b), the circuit can be simplified by combining the parallel current blocking and damping inductors.

When the current blocking and damping inductors are tuned to the resonance frequencies, i.e.

$$L_{h_i} = \frac{1}{\omega_i^2 C_i} \qquad i = \{1, 2, 3, \ldots, n\}, \tag{25}$$

$$L_{b_i} = \frac{1}{\omega_i^2 C_p} \qquad i = \{1, 2, 3, \ldots, n\}. \tag{26}$$

The effective inductance resulting from the parallel connection of (26) and (25) is

$$Z_{L_i}(s) = L_i s = \left(\frac{L_{b_i} L_{h_i}}{L_{b_i} + L_{h_i}}\right) s = L_i s \quad \text{for all } i = \{1, 2, 3, \ldots, n\}. \tag{27}$$

As C_i has been chosen significantly larger than C_p, we have realized a dramatic reduction in the required inductance value. The impedance of the modified series–parallel shunt circuit, as shown in figure7(b), is

$$Z(s) = \sum_{i=1}^{n} \frac{\frac{1}{C_i} s}{s^2 + \frac{1}{R_i C_i} s + \frac{1}{L_i C_i}}. \tag{28}$$

6. Experimental results

6.1. Experimental set-up

As shown in figure 8, the experimental beam is a uniform aluminum bar with rectangular cross section and experimentally pinned boundary conditions at both ends. A pair of piezoelectric ceramic patches (PIC151) are attached symmetrically to either side of the beam surface. One patch is used as an actuator and the other as a shunting layer. Experimental beam and piezoelectric parameters are summarized in tables 1 and 2.

The displacement and voltage frequency responses are measured using a Polytec laser vibrometer (PSV-300) and a HP spectrum analyzer (35670A).

For flexibility during experimentation, the shunt circuits are implemented using a synthetic impedance [13].

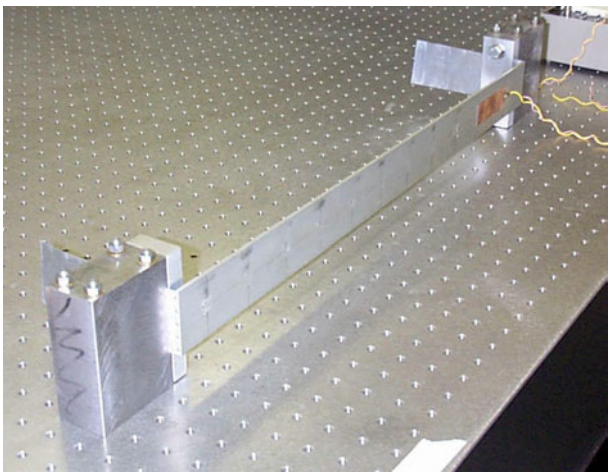

Figure 8. The experimental beam.
(This figure is in colour only in the electronic version)

Table 1. Experimental beam parameters.

Length, L (m)	0.6
Width, w_b (m)	0.05
Thickness, h_b (m)	0.003
Young's modulus, E_b (10^9 N m^{-2})	65
Density, ρ (kg m^{-2})	2650
Piezo location (from end) (m)	0.05 m

Table 2. PZT properties.

Length (m)	0.070
Charge constant, d_{31} (m V^{-1})	-210×10^{-12}
Voltage constant, g_{31} (V m N^{-1})	-11.5×10^{-3}
Coupling coefficient, k_{31}	0.340
Capacitance, C_p (μF)	0.105
Width, $w_s w_a$ (m)	0.025
Thickness, $h_s h_a$ (10^{-3} m)	0.25
Young's modulus, $E_s E_a$ (10^9 N m^{-2})	63

Table 3. Shunt circuit component values.

	Natural PZT	Modified cap.
C_p (nF)	104.8	104.8
C_{ad} (nF)	0	212.2
C_3 (nF)	104.8	317.0
L_1 (H)	41.8	13.9
L_2 (H)	20.8	6.9
L_3 (H)	41.8	13.9
R_1 (Ω)	1543	514
R_1 (Ω)	1145	381

6.2. Supplementary capacitance

A traditional series configuration multi-mode shunt circuit is first designed using the techniques presented in [29] and [2]. A summary of the component values is provided in table 3.

The shunt circuit is then redesigned using a supplementary capacitance of 212.2 nF. A three times reduction of component values is achieved.

A summary of damping performance is provided in table 4. Figure 9 shows the displacement magnitude frequency response for each of the three cases: open loop, shunt damped, and shunt damped with supplementary capacitance.

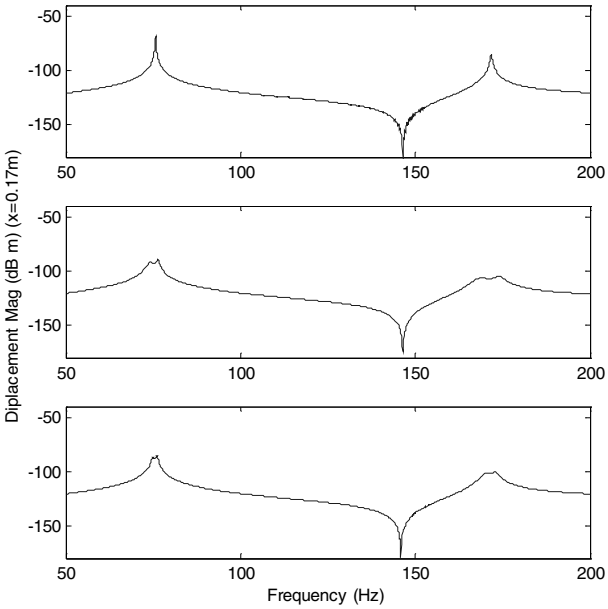

Figure 9. Displacement magnitude frequency response, open loop, shunt damped, and shunt damped with supplementary capacitance. $G_{yv}(s, x = 0.17\text{ m})$.

Table 4. Displacement magnitude reduction.

	Natural PZT	Modified cap.
Second mode (dB)	21.9	18.0
Third mode (dB)	20.4	15.7

Table 5. Component values of the experimental series–parallel shunt circuit.

	Series–parallel	Equivalent value
C_p (nF)	104.8	
C_1 (nF)	1600	
C_2 (nF)	1600	
C_3 (nF)	1600	
L_1 (H)	2.52	41.8
L_2	496 mH	20.8 H
L_3	169 mH	6.8 H
R_1 (kΩ)	60	
R_2 (kΩ)	58	
R_3 (kΩ)	38	

6.3. Series–parallel structure

A series–parallel shunt circuit was designed to damp the second, third, and fourth modes of the experimental beam described in section 6.1. A summary of the circuit components is provided in table 5. The inductor sizes required to implement a traditional resonant shunt circuit or current-flowing shunt circuit are also provided.

The experimental transfer function $G_{vv}(s)$, whose frequency response is shown in figure 10, was measured to allow the simulation of damping performance. The open and closed loop transfer functions, $G_{yv}(s)$ and $\tilde{G}_{yv}(s)$, shown in figure 11, were measured to gauge damping performance. A good correlation was observed between simulated and experimental results. Peak amplitudes of the second, third, and fourth modes were reduced by 15, 12, and 6 dB respectively.

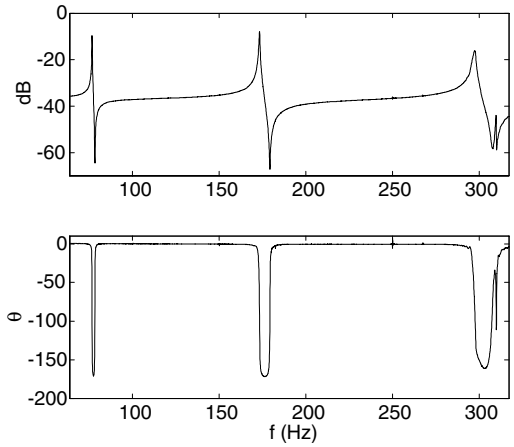

Figure 10. Experimental frequency response from an applied actuator voltage to the resulting open circuit shunt voltage $G_{vv}(\mathrm{j}\omega)$.

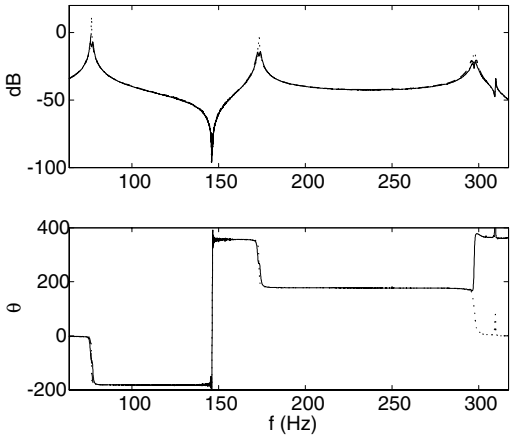

Figure 11. Transfer function from an applied actuator voltage to the measured displacement $G_{yv}(\mathrm{j}\omega)$. Experimental open loop (· · · · · ·), simulated closed loop (——), and experimental closed loop (- - - -).

The time domain response to a low pass filtered step in actuator voltage is shown in figure 12.

7. Conclusions

Structural vibration can be reduced by shunting an attached PZT with an electrical impedance. Current shunt circuit designs require impractically large inductance values of up to thousands of henries.

The size of single- and multi-mode shunt circuit inductors can be reduced by placing an additional capacitance across the terminals of the PZT. Branch inductance and resistance values are reduced by the same factor in which capacitance is increased. Supplementary capacitance also has the consequence of reduced controller gain and damping performance. The situation can be viewed as a trade off between desired component reduction and tolerable performance loss.

Two modes of a simply supported beam are successfully damped using a capacitance modified shunt circuit. The second and third modes of a simply supported beam are reduced in magnitude by 19 and 15.7 dB. These results show

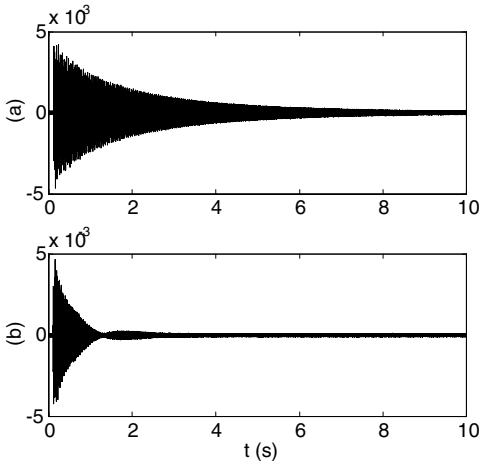

Figure 12. Time domain velocity response of the beam to a low pass filtered step in actuator voltage. Open loop (a), and closed loop (b).

a 3.9 and 4.7 dB reduction in damping performance caused by the introduction of the additional capacitance.

A new type of multi-mode shunt damping circuit has also been introduced. The *series–parallel* impedance structure uses less components, and contains smaller inductors than most previous circuit designs. In comparison with other multi-mode shunt techniques applied to the same experimental beam [3, 12], the series–parallel impedance structure results in less damping, especially at higher frequencies. The loss in performance is due to the method in which adjacent structural modes and circuit networks are decoupled. Unlike other techniques, current from the PZT must flow through all but one of the current blocking networks. The additional complex impedance of each current blocking network, although minor and assumed negligible, sums to significantly disturb the desired impedance at each structural resonance frequency.

Another benefit of the technique introduced is that of simplified tuning. Large valued physical inductors are invariably of fixed design e.g. toroidal core inductors. The interval between available inductance values allows only a coarse tuning of the shunt circuit. As an alternative to varying the inductance values, instead one may tune the arbitrary capacitance values intrinsic to both techniques. Small variable capacitors are widespread and easily obtained.

References

[1] Behrens S, Fleming A J and Moheimani S O R 2001 New method for multiple-mode shunt damping of a structural vibration using a single piezoelectric transducer *Proc. SPIE Smart Structure and Materials, Damping and Isolation (San Diego, CA, March 2001); SPIE* **4331** 239–50

[2] Behrens S and Moheimani S O R 2001 Optimal resistive elements for multiple mode shunt-damping of a piezoelectric laminate beam *Proc. IEEE Conf. on Decision and Control (Sydney, Australia, Dec. 2001)* pp 4018–23

[3] Behrens S and Moheimani S O R 2002 Current flowing multiple mode piezoelectric shunt dampener *Proc. SPIE Smart Materials and Structures (San Diego, CA, March 2002)* pp 4697–24

[4] Behrens S, Moheimani S O R and Fleming A J 2002 Multiple mode passive piezoelectric shunt dampener *Proc. IFAC Mechatronics (Barcelona, 2002)*

[5] Behrens S, Moheimani S O R and Fleming A J 2002 Multiple mode current flowing passive piezoelectric shunt controller *J. Sound Vib.* submitted
[6] Clark W W 2000 Vibration control with state-switched piezoelectric materials *J. Intell. Mater. Syst. Struct.* **11** 263–71
[7] Corr L R and Clark W W 2002 Comparison of low-frequency piezoelectric switching shunt techniques for structural damping *Smart Mater. Struct.* **11** 370–6
[8] Davis C L and Lesieutre G A 2000 An actively tuned solid-state vibration absorber using capacitive shunting of piezoelectric stiffness *J. Sound Vib.* **232** 601–17
[9] Dosch J J, Inman D J and Garcia E 1992 A self-sensing piezoelectric actuator for collocated control *J. Intell. Mater. Syst. Struct.* **3** 166–85
[10] Edberg D L, Bicos A S, Fuller C M, Tracy J J and Fechter J S 1992 Theoretical and experimental studies of a truss incorporating active members *J. Intell. Mater. Syst. Struct.* **3** 333–47
[11] Fleming A J, Behrens S and Moheimani S O R 2000 Synthetic impedance for implementation of piezoelectric shunt-damping circuits *Electron. Lett.* **36** 1525–6
[12] Fleming A J, Behrens S and Moheimani S O R 2002 Optimization and implementation of multi-mode piezoelectric shunt damping systems *IEEE/ASME Trans. Mechatron.* **7** 87–94
[13] Fleming A J, Behrens S and Moheimani S O R 2000 Innovations in piezoelectric shunt damping *Proc. SPIE: Symp. on Smart Materials and MEM's, Smart Structures And Devices (Melbourne, Australia, Dec 2000); SPIE* **4326**
[14] Forward R L 1979 Electronic damping of vibrations in optical structures *Appl. Opt.* **18** 690–7
[15] Fuller C R, Elliott S J and Nelson P A 1996 *Active Control of Vibration* (New York: Academic)
[16] Hagood N W and Von Flotow A 1991 Damping of structural vibrations with piezoelectric materials and passive electrical networks *J. Sound Vib.* **146** 243–68
[17] Hagood N W, Chung W H and von Flowtow A 1990 Modelling of piezoelectric actuator dynamics for active structural control *J. Intell. Mater. Syst. Struct.* **1** 327–54
[18] Hagood N W and Crawley E F 1991 Experimental investigation of passive enhancement of damping for space structures *J. Guid. Control Dyn.* **14** 1100–9
[19] Hollkamp J J 1994 Multimodal passive vibration suppression with piezoelectric materials and resonant shunts *J. Intell. Mater. Syst. Struct.* **5** 49–56
[20] Janocha H 1999 Actuators in adaptronics *Adaptronics and Smart Structures* ed B Clephas (Berlin: Springer) ch 6
[21] Ljung L 1999 *System Identification: Theory for the User* (Englewood Cliffs, NJ: Prentice-Hall)
[22] Meirovitch L 1996 *Elements of Vibration Analysis* 2nd edn (Sydney: McGraw-Hill)
[23] Moheimani S O R, Fleming A J and Behrens S 2002 On the feedback structure of wideband piezoelectric shunt damping systems *Smart Mater. Struct.* **12** 49–56
[24] Moheimani S O R, Fleming A J and Behrens S 2002 On the feedback structure of wideband piezoelectric shunt damping systems *Proc. IFAC World Congr. (Barcelona, Spain, July 2002)* at press
[25] Richard C, Guyomar D, Audigier D and Bassaler H 2000 Enhanced semi-passive damping using continuous switching of a piezoelectric devices on an inductor *Proc. SPIE Smart Structures and Materials, Damping and Isolation (Newport Beach, CA, March 2000); SPIE* **3989** 288–99
[26] Riordan R H S 1967 Simulated inductors using differential amplifiers *Electron. Lett.* **3** 50–1
[27] Won C C 1995 Piezoelectric transformer *J. Guid. Control Dyn.* **18** 96–101
[28] Wu S Y 1996 Piezoelectric shunts with parallel *R–L* circuit for structural damping and vibration control *Proc. SPIE Smart Structures and Materials, Passive Damping and Isolation (March 1996); SPIE* **2720** 259–69
[29] Wu S Y 1998 Method for multiple mode shunt damping of structural vibration using a single PZT transducer *Proc. SPIE Smart Structures and Materials, Smart Structures and Intelligent Systems (Huntington Beach, CA, March 1998); SPIE* **3327** 159–68
[30] Wu S Y 1999 Multiple PZT transducers implemented with multiple-mode piezoelectric shunting for passive vibration damping *Proc. SPIE Smart Structures and Materials, Passive Damping and Isolation (Huntington Beach, CA, March 1999); SPIE* **3672** 112–22
[31] Wu S Y and Bicos A S 1997 Structural vibration damping experiments using improved piezoelectric shunts *Proc. SPIE Smart Structures and Materials, Passive Damping and Isolation (March 1997); SPIE* **3045** 40–50
[32] Zhang J M, Chang W, Varadan V K and Varadan V V 2001 Passive underwater acoustic damping using shunted piezoelectric coatings *Smart Mater. Struct.* **10** 414–20